

Therefore, we regard this paper as only a first step toward understanding the chemistry of metal complexes that deflagrate or explode.

Acknowledgment. We are grateful to Morton-Thiokol, Inc., for financial support of this research on an independent research

and development program and to the Air Force Office of Scientific Research, Aerospace Sciences, with whose support the spectrometer and analytical procedures were developed. We thank Drs. David A. Flanigan, Winston Brundige, Ernest Sutton, and Richard Biddle (Morton-Thiokol) for encouragement and discussions during the course of this work.

Contribution from the Departamentos de Cristalografía y Mineralogía y de Química Inorgánica, Universidad del País Vasco, Apartado 644, 48080 Bilbao, Spain, Sektion für Röntgen- und Elektronenbeugung, Universität Ulm, Oberer Eselsberg, D-7900 Ulm, West Germany, Departamento de Química Inorgánica, Universidad de Valencia, 46100 Burjassot (Valencia), Spain, and Fachbereich Chemie der Universität Marburg, Hans-Meerwein-Strasse, D-3550 Marburg, West Germany

Cu(terpy)X₂ (X = Br⁻, NCS⁻): Complexes with an Unusual Five-Coordination. Structural and Spectroscopic Investigation

M. I. Arriortua,[†] J. L. Mesa,[†] T. Rojo,^{*†} T. Debaerdemaeker,[‡] D. Beltrán-Porter,[§] H. Stratemeier,^{||} and D. Reinen^{*||}

Received May 19, 1987

The structures of the five-coordinate complexes Cu(terpy)X₂ [X = NCS⁻ (I), Br⁻ (II)] were determined (monoclinic, space group C2/c, Z = 4). The unit cell dimensions are *a* = 13.724 (3) [16.818 (3)] Å, *b* = 9.501 (1) [9.280 (10)] Å, *c* = 14.187 (3) [11.396 (7)] Å, β = 110.54 (2)° [125.61 (4)°] for I [II], respectively. The unusual molecular geometry can be understood by following the pathway of the three *ε'* normal modes in D_{3h} symmetry. While usually the pathway leads from the compressed trigonal bipyramid into the elongated square pyramid as the energetically slightly preferred coordination, in these cases a geometry is observed that results from ligand movements in the "reverse" direction. Single-crystal EPR measurements confirmed the structural results and excluded the possibility of a dynamically averaged geometry. In frozen solution a conformational change to a square pyramid occurs.

Introduction

It has been shown that d⁹-configured cations in a chemical environment of five equal ligands tend to stabilize either a compressed trigonal bipyramid or an apically elongated square pyramid with obviously an energetic preference for the latter coordination.¹ Symmetry considerations, based on vibronic interactions between the A₁' ground state and the first excited E' state in D_{3h} via the three *ε'* modes (pseudo-Jahn-Teller effect),² stereochemical results, and angular-overlap energies derived from the electronic spectra were used for the calculation of the ground-state potential surface.³ Three rather flat minima result, which correspond to the three square-pyramidal conformations depicted in Figure 1. The presence of different ligands, rigidity effects of polydentate ligands, or packing effects in the unit cell may modify the potential surface, induced by the pseudo-Jahn-Teller coupling, however, and generate energy minima for geometries different from those just mentioned. The terpyridine ligand in complexes Cu(terpy)X₂·*n*H₂O is interesting in this respect, because it imposes considerable angular distortions and bond length strains on the system. While in Cu(terpy)Cl₂·*n*H₂O (*n* = 0 and 1),^{4,5} in Cu(terpy)(NO₂)₂·H₂O,⁶ and in Cu(terpy)(NO₂)(NO₃)·2H₂O⁷ Cu²⁺ is found in a distorted square pyramid, with the terpyridine ligand in the equatorial plane, the title compounds Cu(terpy)(NCS)₂ and Cu(terpy)Br₂ exhibit a quite unusual coordination geometry in the solid state. The crystal structures and spectroscopic properties are described in this work and will be discussed by utilizing the vibronic coupling with the trigonal-bipyramidal *ε'* normal vibrations.

Experimental Section

Preparation of the Compounds [Cu(terpy)X₂] (X = Br⁻, NCS⁻). X = Br⁻. This compound was synthesized by a method different from the one described in literature.⁴ A solution of CuBr₂ in ethanol (0.86 mmol in 10 mL) was mixed with an ethanol solution containing a stoichiometric

amt. of 2,2':6',2''-terpyridine (0.86 mmol in 15 mL). The microcrystalline green precipitate was washed with ether and recrystallized from a water/ethanol solution. Anal. Found (calcd) for C₁₅H₁₁N₃Br₂Cu: C, 39.3 (39.4); N, 9.3 (9.2); H, 2.2 (2.4); Cu, 13.8 (13.9).

X = NCS⁻. Diluted solutions of CuCl₂·2H₂O in water and terpyridine in ethanol were mixed in a 1:1 molar ratio. The resulting solution was treated with a slight excess of KNCS to give a green precipitate. It was filtered, washed with water, and recrystallized from a water/ethanol solution. Anal. Found (calcd) for C₁₇H₁₁N₅S₂Cu: C, 49.5 (49.4); N, 17.2 (17.0); H, 2.6 (2.7); Cu, 15.4 (15.4).

Spectroscopic Measurements. The ligand field reflection spectra were recorded by a Zeiss PMQII spectrometer (Infrasil) with a low-temperature attachment. We used Sr₂ZnTeO₆ (4000–12000 cm⁻¹) and freshly sintered MgO (8000–30000 cm⁻¹) as standards. The EPR spectra were taken with a Varian E 15 spectrometer (35 and 9 GHz) at 298, 77, and 4.2 K. DPPH was used as internal standard (*g* = 2.003₇).

X-ray Structure Determination. Single crystals of the compounds [Cu(terpy)Br₂] and [Cu(terpy)(NCS)₂], with dimensions 0.5 × 0.04 × 0.02 and 0.35 × 0.14 × 0.11 mm, respectively, were used for crystal data and intensity data collection. Oscillation and Weissenberg photographs were applied to determine the crystal systems. Systematic absences *hkl* (*h* + *k* = 2*n*) and *h0l* (*l* = 2*n*) indicated that the possible space groups are *Cc* or *C2/c* for both complexes. Diffraction data were collected at room temperature on a Philips PW 1100 automated diffractometer, using graphite-monochromated Mo K_α radiation (λ = 0.7107 Å). Physical properties and parameters pertinent to data collection, structure solution, and refinements are reported in Table I.

X = Br⁻. Lattice constants were obtained by a least-squares fit of 30 reflections in the range 4° < 2θ < 50°. Intensities of three standard reflections were measured every 90 min and did not exhibit any significant variations in their intensities during data collection. Correction for Lorentz and polarization effects were applied. Direct methods (MULTAN

- (1) Reinen, D.; Friebe, C. *Inorg. Chem.* **1984**, *23*, 791.
- (2) Pearson, R. G. *Symmetry Rules for Chemical Reactions*; Wiley-Interscience: New York, 1976.
- (3) Reinen, D.; Atanasov, M.; Stratemeier, H. to be submitted for publication.
- (4) Henke, W.; Kremer, S.; Reinen, D. *Inorg. Chem.* **1983**, *22*, 2858.
- (5) Rojo, T.; Vlasse, M.; Beltrán-Porter, D. *Acta Crystallogr., Sect. C: Cryst. Struct. Commun.* **1983**, *C39*, 194.
- (6) Allmann, R.; Kremer, S.; Kucharczyk, D. *Inorg. Chim. Acta* **1984**, *85*, L19.
- (7) Savariault, J. M.; Rojo, T.; Arriortua, M. I.; Galy, J. C. *R. Seances Acad. Sci., Ser. 2* **1983**, *297*, 895.

[†] Universidad del País Vasco.

[‡] Universität Ulm.

[§] Universidad de Valencia.

^{||} Universität Marburg.

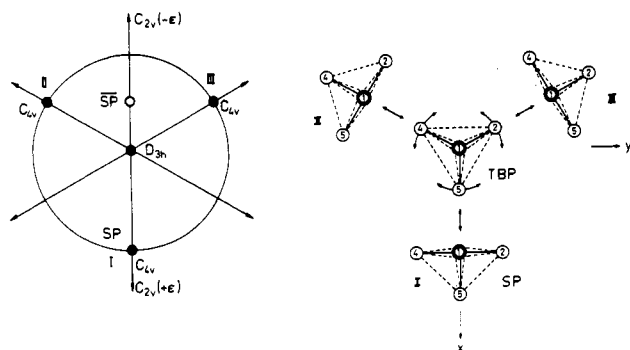


Figure 1. Dynamic averaging process between three square-pyramidal conformations (I-III), which yields the trigonal bipyramid of CuCl_5^{2-} in $[\text{Co}(\text{NH}_3)_6]\text{CuCl}_5^1$ (right). The three square-pyramidal conformations correspond to minima in the ground-state potential surface (left). The distortion paths $+\epsilon$ and $-\epsilon$ in Figure 4 characterize the transitions from the trigonal bipyramid to the square pyramid (SP) and to the "reverse" geometry ($\overline{\text{SP}}$), respectively.

Table I. Physical Properties and Parameters of Data Collection and Refinement

	Crystal Properties	
	$\text{C}_{15}\text{H}_{11}\text{N}_3\text{CuBr}_2$	$\text{C}_{15}\text{H}_{11}\text{N}_3\text{CuN}_2\text{C}_2\text{S}_2$
formula	$\text{C}_{15}\text{H}_{11}\text{N}_3\text{CuBr}_2$	$\text{C}_{15}\text{H}_{11}\text{N}_3\text{CuN}_2\text{C}_2\text{S}_2$
mol wt	456.6	412.7
cryst syst	monoclinic	monoclinic
space group	$C2/c$	$C2/c$
a , Å	16.818 (3)	13.724 (3)
b , Å	9.280 (10)	6.501 (1)
c , Å	11.396 (7)	14.187 (3)
β , deg	125.61 (4)	110.54 (2)
V , Å ³	1446 (5)	1732 (1)
Z	4	4
d_{calcd} , g cm ⁻³	2.09	1.58
d_{obsd} , g cm ⁻³ (by flotation)	2.05 (4)	1.60 (3)
$\mu(\text{Mo K}\alpha)$ cm ⁻¹	72.4	15.5
$F(000)$	884	836
Measurements		
cryst size, mm	$0.5 \times 0.04 \times 0.02$	$0.35 \times 0.14 \times 0.11$
radiation $\lambda(\text{Mo K}\alpha)$, Å	0.7107	0.7107
scan type	$\omega/2\theta$	$\omega/2\theta$
scan speed deg min ⁻¹	1.2	1.2
$2\theta_{\text{max}}$, deg	50	50
hkl range	$h, \pm 16; k, \pm 11; l, \pm 11$	$h, \pm 15; k, \pm 11; l, \pm 15$
data colln range, deg	$4 < 2\theta < 50$	$4 < 2\theta < 50$
Refinements		
no. of reflns obsd	2413	4175
no. of variables (NV)	109	127
no. of reflns used (NO)	$(I \geq 2.5\sigma(I))$	$(I \geq 3\sigma(I))$
$R = \sum [F_o - F_c] / \sum F_o $	0.041	0.048
$R_w = [\sum w(F_o - F_c)^2 / \sum w F_o ^2]^{1/2}$	0.041	0.051

$80)^8$ were applied to solve the structure. In a first step the program yielded the positions of one Cu, one Br, one C, and two N atoms. The positions of all other non-hydrogen atoms were found in subsequent Fourier maps. The structure was refined by a full-matrix least-squares method (SHELX 76).⁹ Anisotropic thermal parameters were used for all the non-H atoms. The hydrogen positions could be derived from a difference Fourier map. Final difference maps revealed no significant regions of electron density with a maximum of 0.42 and a minimum of

Table II. Final Positional and Equivalent Thermal Parameters for $[\text{Cu}(\text{terpy})\text{X}_2]$ ($\text{X} = \text{Br}, \text{NCS}$)

atom	x/a	y/b	z/c	B_{eq} , Å ²
[Cu(terpy)Br ₂]				
Cu	0	0.2778 (1)	0.25	2.176 (4)
N(1)	0.0865 (3)	0.3193 (5)	0.1828 (6)	2.063 (4)
N(2)	0	0.4888 (7)	0.25	1.840 (6)
C(3)	0.1001 (4)	0.4611 (7)	0.1714 (6)	1.703 (8)
C(4)	0.1580 (4)	0.5075 (7)	0.1272 (7)	2.213 (10)
C(5)	0.2030 (5)	0.4013 (8)	0.0983 (7)	2.771 (16)
C(6)	0.1879 (5)	0.2590 (8)	0.1088 (8)	2.827 (9)
C(7)	0.1286 (5)	0.2199 (7)	0.1513 (8)	2.632 (5)
C(8)	0	0.7831 (9)	0.25	2.253 (12)
C(9)	0.0503 (4)	0.7094 (7)	0.2060 (7)	2.089 (6)
C(10)	0.0499 (4)	0.5603 (6)	0.2090 (6)	1.661 (5)
Br(11)	0.1193 (0)	0.1219 (1)	0.4585 (1)	2.729 (4)
[Cu(terpy)(NCS) ₂]				
Cu	0	0.3643 (1)	0.25	2.842 (6)
N(1)	-0.0771 (4)	0.4032 (5)	0.1024 (4)	3.037 (3)
N(2)	0	0.5682 (7)	0.25	2.647 (5)
C(3)	-0.0911 (5)	0.5420 (6)	0.0771 (5)	2.910 (4)
C(4)	-0.1427 (6)	0.5875 (8)	-0.0215 (6)	3.932 (8)
C(5)	-0.1804 (6)	0.4847 (9)	-0.0964 (6)	4.287 (8)
C(6)	-0.1658 (5)	0.3420 (8)	-0.0711 (6)	4.263 (8)
C(7)	-0.1137 (5)	0.3055 (7)	0.0290 (5)	3.600 (4)
C(8)	0	0.8555 (10)	0.25	4.68 (2)
C(9)	-0.0474 (6)	0.7847 (7)	0.1592 (5)	4.05 (1)
C(10)	-0.0460 (5)	0.6380 (7)	0.1627 (5)	3.218 (4)
N(11)	0.1000 (5)	0.2249 (7)	0.2260 (5)	4.482 (8)
C(12)	0.1308 (5)	0.1467 (8)	0.1805 (5)	3.484 (6)
S(13)	0.1775 (2)	0.0372 (2)	0.1186 (2)	5.66 (2)

$$^a B_{\text{eq}} = 8\pi^2[(U_{11} + U_{22} + U_{33})/3].$$

Table III. Bond Distances (Å) for $[\text{Cu}(\text{terpy})\text{Br}_2]$ and $[\text{Cu}(\text{terpy})(\text{NCS})_2]^a$

	[Cu(terpy)Br ₂]	[Cu(terpy)(NCS) ₂]
Cu-N(2)	1.958 (7)	1.937 (7)
Cu-N(1)	2.037 (7)	2.021 (5)
N(2)-C(10)	1.349 (8)	1.350 (7)
C(9)-C(10)	1.384 (9)	1.395 (9)
C(3)-C(10)	1.471 (11)	1.470 (9)
C(8)-C(9)	1.389 (10)	1.395 (8)
N(1)-C(3)	1.355 (8)	1.363 (7)
C(3)-C(4)	1.399 (12)	1.396 (10)
N(1)-C(7)	1.333 (11)	1.353 (8)
C(6)-C(7)	1.387 (15)	1.391 (10)
C(5)-C(6)	1.363 (11)	1.399 (11)
C(4)-C(5)	1.394 (12)	1.402 (11)
Cu-X(11)	2.493 (1)	2.020 (7)
N(11)-C(12)		1.157 (11)
C(12)-S(13)		1.631 (8)

^aX = Br and N (in the NCS group), respectively.

$-0.89 \text{ e } \text{Å}^{-3}$. The scattering factors were taken from ref 10. The best data were obtained for the space group $C2/c$. Final values of the discrepancy indices are $R = 0.041$ and $R_w = 0.041$.

X = NCS⁻. We obtained the dimensions of the monoclinic unit cell by a least-squares fit of 25 reflections in the range $4^\circ < 2\theta < 50^\circ$. No systematic variation of intensity of two standard reflections, measured every 90 min, was observed. The data were corrected for Lorentz and polarization effects. The positional parameters of the heavy atom could be deduced from the Patterson map. The Fourier synthesis then yielded all atoms in the asymmetric unit. H atoms were located and included but not refined. Final difference maps revealed no significant regions of electron density with a maximum of 0.332 and a minimum of $-0.284 \text{ e } \text{Å}^{-3}$. The structure was refined by a full-matrix least-squares method (SHELX 76).⁹ Anisotropic thermal parameters were used for all the non-hydrogen atoms. The refinement in the space group $C2/c$ yielded the discrepancy indices $R = 0.048$ and $R_w = 0.051$.

The final atomic parameters for the compounds $[\text{Cu}(\text{terpy})\text{X}_2]$ ($\text{X} = \text{Br}^-, \text{NCS}^-$) are listed in Table II. Interatomic distances and angles are given in Tables III and IV, respectively.

(8) Main, P.; Fiske, S. J.; Hull, S. E.; Lessinger, L.; Germain, G.; Declercq, J. P.; Woolfson, M. M. "MULTAN 82. A System of Computer Programs for the Automatic Solution of Crystal Structures from X-Ray-Diffraction Data", Universities of York, England, and Louvain, Belgium, 1982.

(9) Sheldrick, G. M. "SHELX 76. Program for crystal structure determination", University of Cambridge, England, 1976.

(10) *International Tables for X-ray Crystallography*; Kynoch: Birmingham, England, 1974; Vol. IV, p 99.

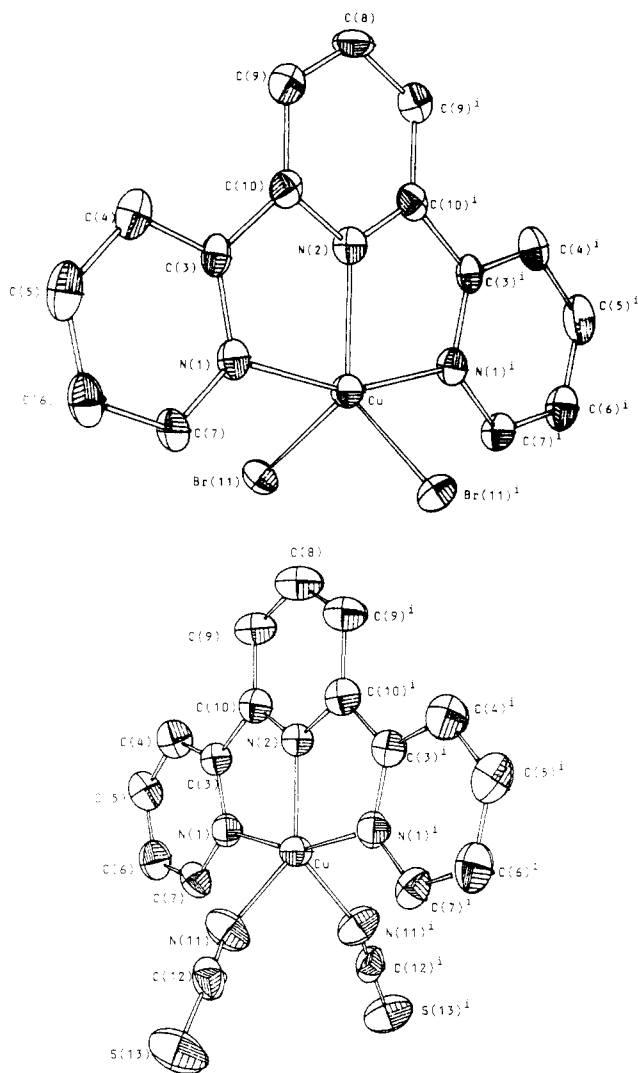


Figure 2. Molecular geometries of $[\text{Cu}(\text{terpy})\text{Br}_2]$ (above) and $[\text{Cu}(\text{terpy})(\text{NCS})_2]$ (below) along the b axis.

Results and Discussion

Structure. Figure 2 shows the molecular geometries and Figure 3 stereodrawings of the unit cells of $\text{Cu}(\text{terpy})(\text{NCS})_2$ and $\text{Cu}(\text{terpy})\text{Br}_2$. The Cu^{2+} ions are coordinated by the three nitrogen atoms of the tridentate terpyridine molecule and the two halide or pseudohalide ions. The latter are bonded to Cu^{2+} via the nitrogen atoms. Each molecule lies astride a crystallographic 2-fold axis (through $\text{C}(8)\text{--N}(2)\text{--Cu}$), which is also the direction of the b axis. The coordination polyhedra with the symmetry C_{2v} correlate neither with a trigonal bipyramid nor with a square pyramid. The average $\text{Cu}\text{--N}$ distances between Cu^{2+} and the

Table IV. Bond Angles (deg) for $[\text{Cu}(\text{terpy})\text{Br}_2]$ and $[\text{Cu}(\text{terpy})(\text{NCS})_2]^a$

	$[\text{Cu}(\text{terpy})\text{Br}_2]$	$[\text{Cu}(\text{terpy})(\text{NCS})_2]$
$\text{N}(1)\text{--Cu--N}(2)$	79.1 (1)	79.5 (1)
$\text{Cu--N}(2)\text{--C}(10)$	119.5 (4)	119.4 (4)
$\text{N}(2)\text{--C}(10)\text{--C}(9)$	120.9 (7)	121.3 (6)
$\text{N}(2)\text{--C}(10)\text{--C}(3)$	111.8 (5)	112.2 (6)
$\text{C}(3)\text{--C}(10)\text{--C}(9)$	127.3 (7)	126.4 (6)
$\text{C}(10)\text{--N}(2)\text{--C}(10)^i$	121.1 (6)	121.2 (6)
$\text{C}(8)\text{--C}(9)\text{--C}(10)$	118.1 (8)	116.9 (6)
$\text{C}(9)\text{--C}(8)\text{--C}(9)^i$	121.0 (7)	122.4 (8)
$\text{N}(1)\text{--C}(3)\text{--C}(10)$	115.0 (7)	113.8 (5)
$\text{C}(4)\text{--C}(3)\text{--C}(10)$	123.4 (6)	123.6 (6)
$\text{N}(1)\text{--C}(3)\text{--C}(4)$	121.7 (7)	122.6 (6)
$\text{Cu--N}(1)\text{--C}(3)$	114.6 (5)	115.1 (4)
$\text{Cu--N}(1)\text{--C}(7)$	125.3 (5)	126.1 (4)
$\text{C}(3)\text{--N}(1)\text{--C}(7)$	120.0 (7)	118.8 (5)
$\text{N}(1)\text{--Cu--N}(1)^i$	158.2 (2)	158.9 (2)
$\text{N}(1)\text{--C}(7)\text{--C}(6)$	121.0 (6)	122.2 (6)
$\text{C}(5)\text{--C}(6)\text{--C}(7)$	119.5 (8)	118.7 (7)
$\text{C}(4)\text{--C}(5)\text{--C}(6)$	120.6 (9)	119.9 (7)
$\text{C}(3)\text{--C}(4)\text{--C}(5)$	117.0 (6)	117.8 (7)
$\text{N}(2)\text{--Cu--X}(11)$	125.5 (0)	130.9 (2)
$\text{N}(1)\text{--Cu--X}(11)$	96.5 (1)	98.9 (2)
$\text{X}(11)\text{--Cu--X}(11)^i$	109.0 (0)	98.1 (3)
$\text{Cu--N}(11)\text{--C}(12)$		156.6 (5)
$\text{N}(11)\text{--C}(12)\text{--S}(13)$		178.4 (6)

^a X = Br and N (in the NCS group), respectively. Symmetry operation: $i = -x, y, 1/2 - z$.

terpyridine ligand ($\approx 2.00 \text{ \AA}$) in both complexes are similar to those in $\text{Cu}(\text{terpy})\text{Cl}_2 \cdot n\text{H}_2\text{O}$ ($n = 0, 1$).^{4,5} But while the two $\text{Cu}\text{--Cl}$ spacings in the latter compounds differ by more than 0.2 \AA , corresponding to a distorted square pyramid with a very long apical bond distance, the two $\text{Cu}\text{--Br}(11)$ or $\text{Cu}\text{--N}(11)$ bonds are of equal length in the two complexes under discussion. The angles between Cu^{2+} and the two $\text{Br}(11)$ [$\text{N}(11)$] atoms, which lie in one plane with the $\text{N}(2)$ atom of the terpyridine ligand, are remarkably small at 109° (98°).

The observed geometry is extraordinary for five-coordinate species. The unexpected geometry can be verified, however, if vibronic interactions via the ϵ' modes in D_{3h} symmetry are considered.^{1,3} Starting with a trigonal bipyramid, which is usually axially compressed if observed with Cu^{2+} as the central ion,¹ the ϵ components of the stretching and the two deformation ϵ' modes transform the molecule into a polyhedron with C_{2v} symmetry (Figure 4). Without steric ligand constraints or geometrical packing effects in the unit cell, the complex moves toward an elongated square pyramid.^{1,3} The "reverse" movement of the ligands would lead into a geometry which closely resembles that observed for $\text{Cu}(\text{terpy})\text{X}_2$ [$\text{X} = \text{NCS}^-, \text{Br}^-$] (Figure 2). In these conformations the $\text{Cu}\text{--N}(2)$ spacings are shorter than the $\text{Cu}\text{--N}(1)$ bond lengths, and the two $\text{N}(1)$ ligator atoms are bent toward the $\text{Cu}\text{--N}(2)$ bond. A decrease of the $\text{Br}\text{--Cu}\text{--Br}^i$ and $\text{N}(11)\text{--Cu}\text{--N}(11)^i$ angles below 120° , and comparatively long $\text{Cu}\text{--N}(11)$ and $\text{Cu}\text{--Br}$ spacings are also expected in this steric

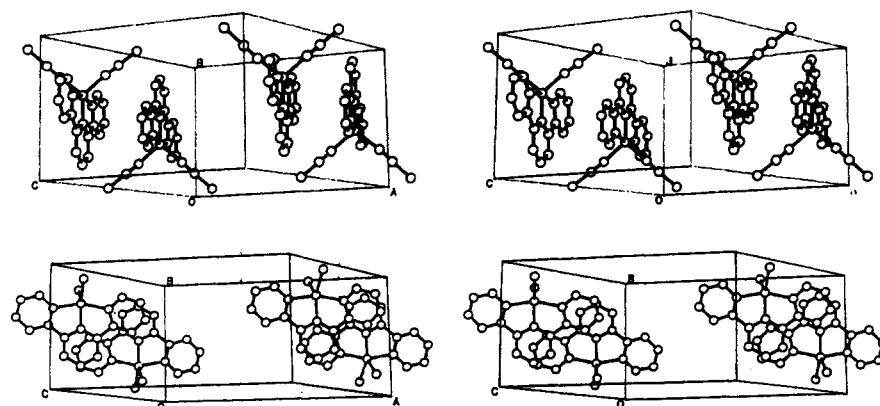


Figure 3. Stereoscopic views of the unit cells of $[\text{Cu}(\text{terpy})(\text{NCS})_2]$ (above) and $[\text{Cu}(\text{terpy})\text{Br}_2]$ (below).

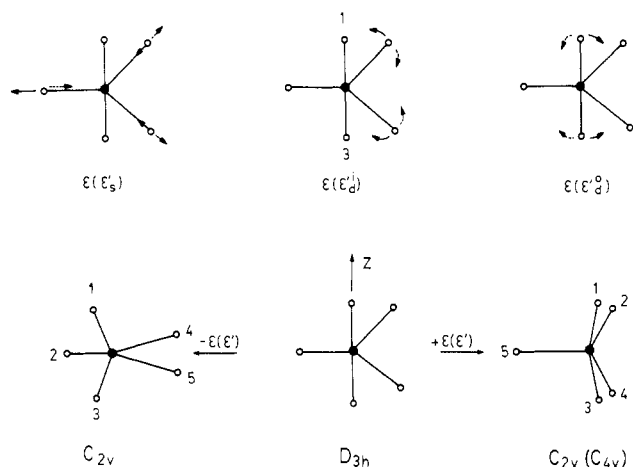


Figure 4. ϵ components of the three ϵ' vibrational modes in D_{3h} (stretching, in-plane and out-of-plane deformations) (above) and the distortions induced by linear combinations of these components (below). For Cu(terpy)X_2 : [1, 3 \equiv N(1), N(1)ⁱ; 2 \equiv N(2)]; (a) $-\epsilon(\epsilon')$ [(X = Br⁻ (NCS⁻); 4, 5, \equiv Br, Brⁱ (N(11), N(11)ⁱ)] (C_2 axis follows the Cu–N(2) direction); (b) $+\epsilon(\epsilon')$ (X = Cl⁻; 4, 5 \equiv Cl, 4 \equiv Clⁱ) (C_2 axis follows either one of the two Cu–Cl bond directions).

conformation (Figure 4), in agreement with the structural results (Tables III and IV).

The molecular structure of Co(terpy)(NCO)_2 ¹¹ also shows the features of a "reverse" geometry, though the deviation from the trigonal bipyramid is much less pronounced. Zn(terpy)(NCS)_2 presumably has the same molecular structure (see below). Because Co^{2+} (as Zn^{2+}) does not undergo a Jahn–Teller-type vibronic coupling and the N-ligand atoms in NCS^- and NCO^- have very similar bonding properties, we may conclude that the rigidity of the terpyridine ring (and the presence of different ligands) are reflected by the geometry of the Co^{2+} polyhedron. Though the pseudo-Jahn–Teller effect mainly induces the large deviations from the trigonal-bipyramidal parent geometry of five-coordinate Cu^{2+} complexes,^{1,3} the steric constraints of the terpyridine ligand apparently stabilize the specific "reverse geometry" of the CuN_3Br_2 and $\text{CuN}_3\text{N}'_2$ polyhedra.

The described "reverse geometry" may also be looked at as the intermediate between two elongated square pyramids, in which the apical position is alternatively occupied by one of the two NCS^- or Br^- ligands (Figure 1). If the angles θ and ϕ in the square pyramid are 165° (SP, Figure 5), following the pseudorotation from D_{3h} to C_{4v} (Figure 4) ($\theta = 180^\circ \rightarrow 180^\circ - 15^\circ$; $\phi = 120^\circ \rightarrow 120^\circ + 45^\circ$), they should be $\theta = 180^\circ + 7.5^\circ = 187.5^\circ$ and $\phi = 120^\circ - 22.5^\circ = 97.5^\circ$ for the intermediate or reverse geometry ($\overline{\text{SP}}$). The latter angle is the one observed for Cu(terpy)(NCS)_2 , while θ is fixed by the rigidity of the terpyridine ligand and is larger than expected (Table IV: 159° or 201°).

In Figure 5 a series of compounds $\text{Cu(terpy)XX}'$ and the idealized D_{3h} and C_{4v} coordination polyhedra are geometrically characterized by the angles ν_5 and ν_4 , with a fixed bite angle $\text{N}(1)\text{--Cu--N}(1)^i$ (electron-pair repulsion approach¹²). Most $\text{Cu(terpy)XX}'$ entities are obviously square pyramids in fair approximation; the two compounds under discussion have positions in the $\nu_5\text{--}\nu_4$ plane very near to $\overline{\text{SP}}$ or "halfway" between this and the trigonal bipyramid, in accord with the statements above. Complex 3 with a CuN_3O_2 coordination¹³ possesses a geometry

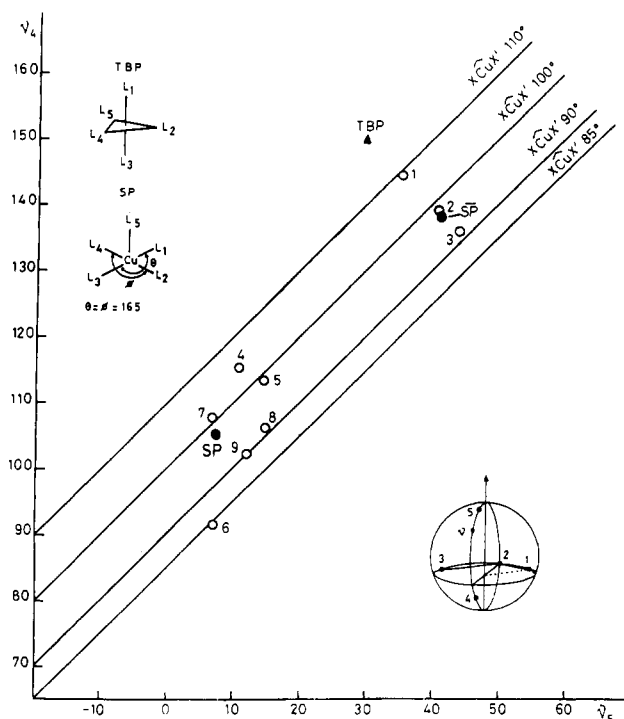


Figure 5. Diagram characterizing the geometry of five-coordinate complexes $\text{Cu(terpy)XX}'$ in comparison to idealized polyhedra of the symmetries D_{3h} and C_{4v} (X and X' in positions 5 and 4; $\overline{\text{SP}}$ is explained in the text and Figures 1 and 4): (1) Cu(terpy)Br_2 ; (2) Cu(terpy)(NCS)_2 ; (3) Cu(terpy)(tda) ; (4) Cu(terpy)Cl_2 ; (5) $[\text{Cu(terpy)CN}](\text{NO}_3 \cdot \text{H}_2\text{O})$; (6) $[\text{Cu(terpy)(ONO)OH}_2](\text{NO}_2 \cdot \text{H}_2\text{O})$; (7) $\text{Cu(terpy)Cl}_2 \cdot \text{H}_2\text{O}$; (8) $[\text{Cu(terpy)Br}](\text{PF}_6)$; (9) $[\text{Cu(terpy)Cl}](\text{PF}_6)$.

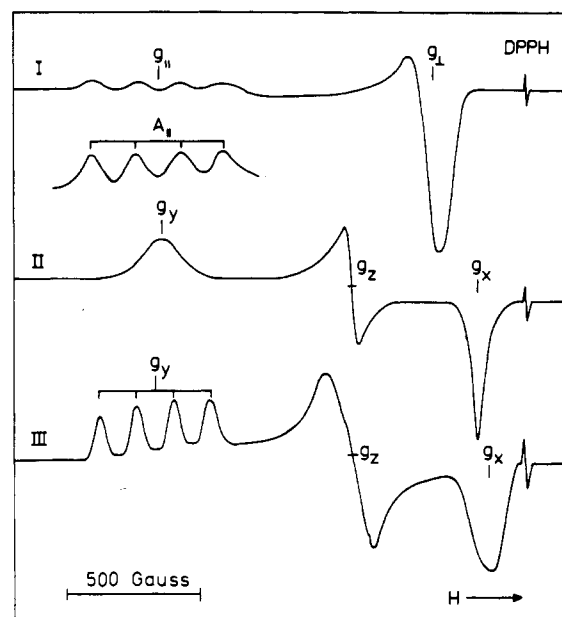


Figure 6. Q-Band EPR spectra of Cu(terpy)(NCS)_2 -frozen DMF solution at 130 K (I), Cu(terpy)(NCS)_2 powder at 4.2 K (II), and Cu^{2+} -doped Zn(terpy)(NCS)_2 powder at 77 K (III).

very similar to the one of Cu(terpy)(NCS)_2 , but with a $\text{O--Cu--O}'$ angle (92°) that is even smaller than the angle $\text{N}(11)\text{--Cu--N}(11)^i$ (98°) in the latter compound.

Spectroscopy. The powder EPR spectra of Cu(terpy)X_2 [X = NCS^- , Br^-] are strongly orthorhombic (Figure 6) and remain

- (11) Kepert, D. L.; Kucharski, E. S.; White, A. H. *J. Chem. Soc., Dalton Trans.* **1980**, 1932.
 (12) Kepert, D. L. *Inorganic Stereochemistry*; Springer West Berlin, 1982.
 (13) Bonomo, R. P.; Rizzarelli, E.; Bresciani-Pahor, N.; Nardin, G. *J. Chem. Soc., Dalton Trans.* **1982**, 681.
 (14) Anderson, O. P.; Packard, A. B.; Wicholas, M. *Inorg. Chem.* **1976**, *15*, 1613.
 (15) Rojo, T.; Arriortua, M. I.; Mesa, J. L.; Cortes, R.; Darriet, J.; Villeneuve, G.; Beltrán-Porter, D. *Inorg. Chim. Acta* **1987**, *134*, 59.
 (16) Rojo, T.; Arriortua, M. I.; Ruiz, J.; Darriet, J.; Villeneuve, G.; Beltrán-Porter, D. *J. Chem. Soc., Dalton Trans.* **1987**, 285.

- (17) In contrast to the dynamically averaged trigonal bipyramid of CuCl_5^{2-} , one conformation is excluded from the pseudorotation (Figure 1), because the imposed short Cu–N(2) spacing makes an elongation along this bond direction energetically unfavorable.

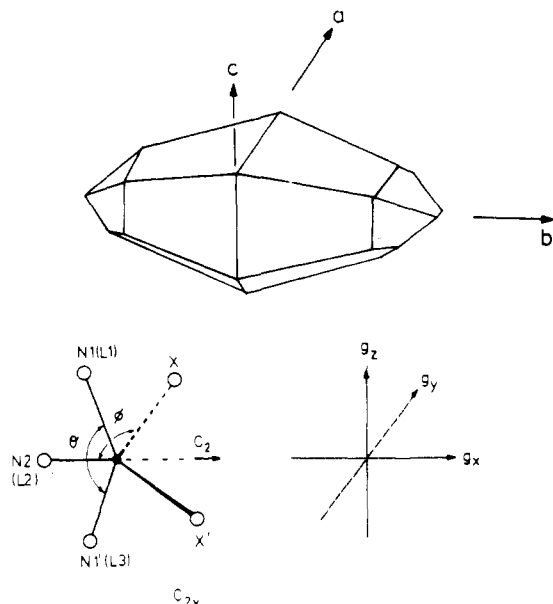


Figure 7. Crystal shape and orientations of the crystallographic axes (above) and the correlation of the molecular geometry of the CuN_3X_2 polyhedron with the directions of the g tensor components (below) for $\text{Cu}(\text{terpy})(\text{NCS})_2$.

practically unchanged in dependence on temperature [$g_x = 2.03_3$ (2.03₀), $g_z = 2.11_7$ (2.11₅), and $g_y = 2.25_1$ (2.25₆) at 298 (4.2) K for the thiocyanate and $g_x = 2.03_2$ (2.03₀), $g_z = 2.12_6$ (2.12₂), and $g_y = 2.23_9$ (2.23₈) at 298 (4.2) K for the bromide]. Cu^{2+} -doped $\text{Zn}(\text{terpy})(\text{NCS})_2$ has practically the same g values as $\text{Cu}(\text{terpy})(\text{NCS})_2$, but with a well-resolved hyperfine structure in the g_y signal (Figure 6; $A_{\parallel} = 146 \times 10^4 \text{ cm}^{-1}$).

The four formula units in the unit cell are magnetically equivalent, and hence only one EPR signal is observed in the single-crystal experiment. A single crystal of $\text{Cu}(\text{terpy})(\text{NCS})_2$ with the shape shown in Figure 7 was used. The angular dependencies of the g tensor at 298 K were measured in three mutually perpendicular planes (Figure 8). g_x ($=2.03_2$) is correlated with the Cu–N(2) bond direction. The g_z component ($=2.11_3$) is located in the plane of the (Cu(terpy)) fragment at an angle of $\approx 35^\circ$ with respect to the c axis (Figure 8), in agreement with the crystallographic angle ($\approx 30^\circ$) within the experimental adjustment uncertainty. g_y ($=2.25_0$) finally lies in the N(11)–Cu–N(11)ⁱ plane perpendicular to the molecular C_2 axis.

The ground-state wave function of a five-coordinate Cu^{2+} complex along the $\pm e$ distortion coordinate (Figures 1 and 4) is³

$$\varphi_g = (1 + c)^{-1/2} \{d_{z^2} + cd_{x^2-y^2}\} \quad (1)$$

The mixing coefficient is $c = 0$ for the trigonal bipyramid (d_{z^2} ground state) and $c = 1/3^{1/2}$ for the square pyramid with a $d_{x^2-y^2}$ ground state. Negative c coefficients would correspond to ligand displacements in the "reverse" direction. The experimental g values for the thiocyanate are exactly reproduced with $c = -3^{1/2}/2$, utilizing eq 2,³ and the ground state is "very near" to $d_{z^2-x^2}$ ($c = -1/3^{1/2}$):

$$g_z = g_0 + 8u_z \frac{c^2}{1 + c^2}$$

$$g_{x(y)} = g_0 + 2u_{x(y)} \frac{c^2}{1 + c^2} \left(1 + \frac{3^{1/2}}{c} \right)^2 \quad (2)$$

with

$$u_i = \frac{k_i^2 \xi_0}{\Delta_i} \quad (i = x, y, z)$$

k_i and ξ_0 ($=830 \text{ cm}^{-1}$) are covalency factors and the spin-orbit

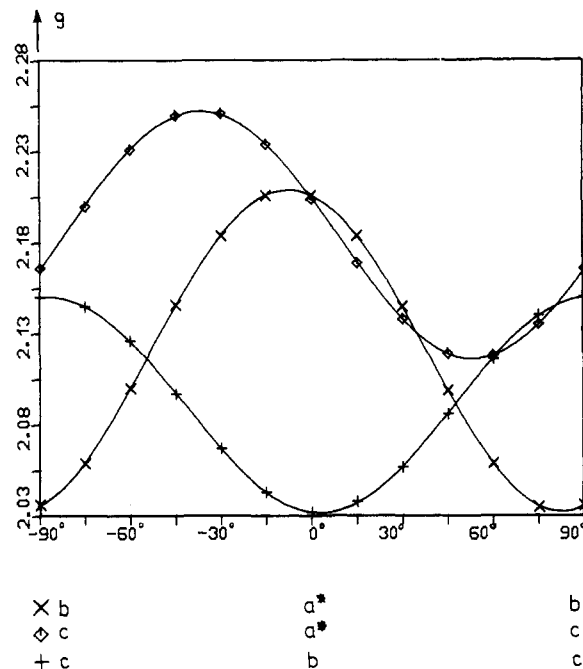


Figure 8. Angular dependence of the g tensor of $\text{Cu}(\text{terpy})(\text{NCS})_2$ in three mutually perpendicular planes (a^* is defined \perp to b, c). For orientations, see Figure 7.

coupling parameter for the free Cu^{2+} ion, respectively. The Δ_i energies are the d–d transitions ${}^2A_1(\approx d_{z^2-x^2}) \rightarrow {}^2B_2(d_{xz})$, ${}^2B_1(d_{xy})$, and ${}^2A_2(d_{yz})$ for $i = y, z$, and x in C_{2v} symmetry. They were derived from the ligand field reflection spectrum of $\text{Cu}(\text{terpy})(\text{NCS})_2$. The spectrum shows but one very broad asymmetric band around 13500 cm^{-1} at 298 K, which is resolved into two transitions at 10500 and 13750 cm^{-1} at 4.2 K, however, with the latter of slightly higher intensity. We assign the higher energy band to the three closely spaced transitions (from which the one to 2A_2 is symmetry forbidden) needed for the evaluation of the orbital contributions of the g values and the former to the ${}^2A_1(\approx d_{z^2-x^2}) \rightarrow {}^2A_1$ (mainly d_{yz}) transition. The derived covalency factor $k_x \approx k_y \approx k_z \approx 0.74$ is of the expected magnitude for nitrogen ligator atoms. The band energies and intensity distribution are similar to those of $\text{Cu}(\text{terpy})\text{Cl}_2$, though the molecular geometry is a distorted square pyramid in the chloride.⁴ This result supports the argument of rather similar energies for the different conformational geometries, which characterize the ground-state potential surface of five-coordinate complexes.³

So far, our considerations refer to a static molecular structure. If the polyhedron geometry would be the dynamic average over two square-pyramidal conformations,¹⁷ a different g tensor would be expected

$$g_{\parallel}^d \approx g_0 + 2u \quad g_{\perp}^d \approx g_0 + 5u \quad (3)$$

in contrast to the experiment. It results from eq 2 with $c = 1/3^{1/2}$ (polyhedron I: $g_x = g_0 + 8u$; $g_y = g_z = g_0 + 2u$) and—after transformation of I to II (III)—by motional narrowing between polyhedra II and III in the xy plane (Figure 1). Apparently the "reverse" geometry with ligand displacements leading to rather short Cu–L(2) spacings and to a L(4)–Cu–L(5) angle around 100° as well as to Cu–L(1) and Cu–L(3) bonds that are bent toward the Cu–L(2) bond direction (Figure 4), is statically stabilized. The minima connected with the elongated square pyramids II and III collapse to a new minimum in the ground-state potential surface at the $\overline{\text{SP}}$ position. This effect is due to the specific ligand strain, which is directly evident in the molecular structure of $\text{Co}(\text{terpy})(\text{NCO})_2$,¹¹ as already mentioned. The same conclusion comes from the EPR spectrum of Cu^{2+} -doped $\text{Zn}(\text{terpy})(\text{NCS})_2$ (Figure 6), which is presumably isostructural with $\text{Co}(\text{terpy})(\text{NCO})_2$. The presence of different ligands in $\text{M}^{\text{II}}(\text{terpy})\text{X}_2$ complexes may alter the strain by additional bonding anisotropies. $\text{Zn}(\text{terpy})\text{Cl}_2$ for example is dimorphous. In one modification the

polyhedron geometry¹⁸ is similar to that of Co(terpy)(NCO)₂, in the other the polyhedron is approximately a square pyramid.¹⁹ This finding may explain that Cu(terpy)Cl₂—in contrast to the thiocyanate and the bromide complexes—has a different geometry, namely a strongly elongated square pyramid.^{4,5} We have also measured the EPR spectra of the two complexes (130 K) in frozen DMF and DMSO solutions but did not succeed in obtaining signals in more nonpolar solvents for solubility reasons. Surprisingly, completely different *g* tensors from those in the solid state were obtained. They are tetragonal within the line width for the thiocyanate (Figure 6) and only slightly orthorhombic for the bromide. Both spectra are strongly indicative of (approximately) square-pyramidal geometries [*g*_{||} = 2.25₆ (2.26₅), *g*_⊥ = 2.06₄ (≈2.05) for *x* = NCS⁻(Br⁻)]. The average *g* value is slightly smaller in the matrix than in the solid state. The *A*_{||} value from the well-resolved hyperfine splitting in the *g*_{||} signal of Cu(terpy)(NCS)₂ (-172 × 10⁻⁴ cm⁻¹) is significantly larger than the one in the orthorhombic *g*_⊥ signal of Cu²⁺-doped Zn(terpy)(NCS)₂ (-147 × 10⁻⁴ cm⁻¹; Figure 6). The derived mixing coefficient *α* of the d_{2-y²} orbital in the ground-state MO yields 0.87, in good agreement with the coefficient for Cu(II)-nitro complexes.²⁰ *A*_{||} (= -178 cm⁻¹) is slightly larger for the bromide. The solution and solid solution ligand field spectra exhibit a band at 14 900 cm⁻¹ with a weak shoulder around 12 000 cm⁻¹, at about 10% higher energy than in case of the \overline{SP} geometry. Apparently the energy, which determines the conformational change in going from the solid state to matrix isolation, is only very small. Alternatively the square-pyramidal geometry in solid solution may have been stabilized by a very weakly bonded solvent molecule in the free axial position.

Conclusions

The singular molecular geometries of the five-coordinate Cu(terpy)X₂ complexes with X = NCS⁻ and Br⁻ (Figure 2) can be rationalized by following a pathway that classifies the ligand displacements corresponding to the three *ε'* vibrations in *D*_{3h} symmetry (Figures 1 and 4).³ The (A₁' + E') ⊗ *ε'* vibronic coupling calculations for the CuCl₅³⁻ model complex yield a ground-state potential surface that possesses minima for three equivalent C_{2v} geometries (nearly C_{4v} elongated square pyramids; see Figure 1) and three saddle points also with C_{2v} symmetry in the "reverse" directions (between the C_{4v} minima in Figure 1). The energy differences between the elongated square pyramid, the "reverse" geometry, and the compressed trigonal bipyramid are usually small and may even fall into the range of thermal energies.³ It is hence apparently possible to stabilize any coordination along the *ε'* pathways with C_{2v} or even lower symmetries if steric ligand strains, the presence of different ligands, packing effects in the unit cell, or weak solvent effects are additionally present. For the two complexes under discussion, the specific geometry of the rigid terpyridine ligand seems to have been deciding for the stabilization of a geometry along the displacement coordinate in the "reverse" direction. There is no convincing evidence, either from EPR spectroscopy or from anomalous temperature ellipsoids of Cu²⁺ and the nitrogen and bromide ligator atoms, that the observed molecular geometries are dynamically averaged square-pyramidal conformations.

Acknowledgment. This work was supported in part by Grant 2930/83 from the CAICYT and by the "Deutsche Forschungsgemeinschaft", which we gratefully acknowledge.

Registry No. [Cu(terpy)Br₂], 25971-38-4; [Cu(terpy)(NCS)₂], 25970-65-4; [Zn(terpy)(NCS)₂], 115560-02-6.

Supplementary Material Available: Table S1 (anisotropic thermal parameters) and Table S2 (hydrogen coordinates and the C-H distances) (2 pages); Table S3 (calculated and observed structure factors) (9 pages). Ordering information is given on any current masthead page.

- (18) Vlasse, M.; Rojo, T.; Beltran-Porter, D. *Acta Crystallogr., Sect. C: Cryst. Struct. Commun.* **1983**, C39, 560.
 (19) Einstein, F. W. B.; Penfold, B. R. *Acta Crystallogr.* **1966**, 20, 924.
 (20) Ozarowski, A.; Reinen, D. *Inorg. Chem.* **1985**, 24, 3860.

Contribution from the Departments of Chemistry, Tokyo Institute of Technology, O-okayama, Meguro-ku, Tokyo 152, Japan, and Ochanomizu University, Otsuka, Bunkyo-ku, Tokyo 112, Japan

Crystal Structure and Absolute Configuration of (+)₂₇₅^{CD}-Tris(2,4-pentanedionato)ruthenium(III)

Hideyo Matsuzawa,[†] Yuji Ohashi,[‡] Youkoh Kaizu,[†] and Hiroshi Kobayashi^{*†}

Received February 9, 1988

The crystal structure and absolute configuration of (+)₂₇₅^{CD}-tris(2,4-pentanedionato)ruthenium(III) ((+)₂₇₅^{CD}-[Ru(acac)₃]) have been determined from the single-crystal X-ray data. The red crystals of (+)₂₇₅^{CD}-[Ru(acac)₃] obtained by condensation of the first fraction eluted by hexane/propanol from a high-performance liquid chromatography (HPLC) column of porous silica gel coated with cellulose tris(phenylcarbamate) are monoclinic with unit-cell dimensions *a* = 12.750 (3) Å, *b* = 12.540 (2) Å, *c* = 11.435 (3) Å, *β* = 101.17 (3)°, *V* = 1793.7 Å³, space group *P*2₁, and *Z* = 4. The structure was solved by direct methods and refined to *R* = 0.046. (+)₂₇₅^{CD}-[Ru(acac)₃] has a Δ configuration of *D*₃ symmetry with a very slight axial elongation.

Introduction

In a previous work, we achieved a complete resolution of the enantiomeric isomers of [Ru(acac)₃] (acac = 2,4-pentanedionate) by high-performance liquid chromatography (HPLC) on a column of porous silica gel coated with cellulose tris(phenylcarbamate). The antipodes in the first and the second fractions ((+)₂₇₅^{CD}- and (-)₂₇₅^{CD}-[Ru(acac)₃]) eluted by hexane/propanol were assigned the configurations Δ and Λ, respectively.¹ Our assignment was based on the theoretically predicted circular dichroism (CD) in the intense ligand (π,π*) exciton band at around 36 × 10³ cm⁻¹. The assignment is supported by the observed CD sign of partly resolved

[Ru(acac)₃] with the Δ isomer in excess² and also by those observed for completely resolved Δ-trans, Δ-cis and Λ-trans, Λ-cis diastereomers of [Ru(+-)-atc]₃ ((+)-atc = (+)-3-acetyl camphorate), respectively.³

The CD spectrum of [Ru(acac)₃] shows an extremum in the lowest ligand (π,π*) band in contrast with the well-resolved dispersions observed in the ligand band of the corresponding enantiomeric isomers of chromium(III), cobalt(III), and rhodium(III) analogues.^{2a} The same phenomenon was observed with

[†] Tokyo Institute of Technology.
[‡] Ochanomizu University.

- (1) Kobayashi, H.; Matsuzawa, H.; Kaizu, Y.; Ichida, A. *Inorg. Chem.* **1987**, 26, 4318.
 (2) (a) Mason, S. F.; Peacock, R. D.; Prosperi, T. *J. Chem. Soc., Dalton Trans.* **1977**, 702. (b) Drake, A. F.; Gould, J. M.; Mason, S. F.; Rosini, C.; Woodley, F. J. *Polyhedron* **1983**, 2, 537.
 (3) Everett, G. W., Jr.; King, R. M. *Inorg. Chem.* **1972**, 11, 2041.